

## Syngas production by electrocatalytic reduction of CO<sub>2</sub> using Ag-decorated TiO<sub>2</sub> nanotubes

Farkhondehfal, M. A.; Hernández, S.; Rattalino, M.; Makkee, M.; Lamberti, A.; Chiodoni, A.; Bejtka, K.; Sacco, A.; Pirri, F. C.; Russo, N.

### DOI

[10.1016/j.ijhydene.2019.04.180](https://doi.org/10.1016/j.ijhydene.2019.04.180)

### Publication date

2019

### Document Version

Final published version

### Published in

International Journal of Hydrogen Energy

### Citation (APA)

Farkhondehfal, M. A., Hernández, S., Rattalino, M., Makkee, M., Lamberti, A., Chiodoni, A., Bejtka, K., Sacco, A., Pirri, F. C., & Russo, N. (2019). Syngas production by electrocatalytic reduction of CO<sub>2</sub> using Ag-decorated TiO<sub>2</sub> nanotubes. *International Journal of Hydrogen Energy*, 45(50), 26458-26471. <sup>2</sup>  
<https://doi.org/10.1016/j.ijhydene.2019.04.180>

### Important note

To cite this publication, please use the final published version (if applicable).  
Please check the document version above.

### Copyright

Other than for strictly personal use, it is not permitted to download, forward or distribute the text or part of it, without the consent of the author(s) and/or copyright holder(s), unless the work is under an open content license such as Creative Commons.

### Takedown policy

Please contact us and provide details if you believe this document breaches copyrights.  
We will remove access to the work immediately and investigate your claim.

***Green Open Access added to TU Delft Institutional Repository***

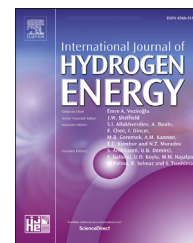
***'You share, we take care!' – Taverne project***

***<https://www.openaccess.nl/en/you-share-we-take-care>***

Otherwise as indicated in the copyright section: the publisher is the copyright holder of this work and the author uses the Dutch legislation to make this work public.

Available online at [www.sciencedirect.com](http://www.sciencedirect.com)

ScienceDirect

journal homepage: [www.elsevier.com/locate/he](http://www.elsevier.com/locate/he)

# Syngas production by electrocatalytic reduction of CO<sub>2</sub> using Ag-decorated TiO<sub>2</sub> nanotubes

M.A. Farkhondehfal <sup>b,\*</sup>, S. Hernández <sup>a,\*\*</sup>, M. Rattalino <sup>a</sup>, M. Makkee <sup>c</sup>,  
A. Lamberti <sup>a</sup>, A. Chiodoni <sup>b</sup>, K. Bejtka <sup>b</sup>, A. Sacco <sup>b</sup>, F.C. Pirri <sup>a,b</sup>, N. Russo <sup>a</sup>

<sup>a</sup> Department of Applied Science and Technology, Politecnico di Torino, Turin, Italy

<sup>b</sup> Center for Sustainable Future Technologies (CSFT@POLITO), Istituto Italiano di Tecnologia, Turin, Italy

<sup>c</sup> Catalysis Engineering, Dept. of Chemical Engineering, Faculty of Applied Sciences, Delft University of Technology, Delft, the Netherlands

## ARTICLE INFO

### Article history:

Received 11 March 2019

Received in revised form

14 April 2019

Accepted 17 April 2019

Available online xxx

### Keywords:

Electrocatalyst

CO<sub>2</sub> reduction

Titania nanotube

Silver nano particles

Electrochemical surface area

## ABSTRACT

Huge efforts have been done in the last years on electrochemical and photoelectrochemical reduction of CO<sub>2</sub> to offer a sustainable route to recycle CO<sub>2</sub>. A promising route is to electrochemically reduce CO<sub>2</sub> into CO which, by combination with hydrogen, can be used as a feedstock to different added-value products or fuels. Herein, perpendicular oriented TiO<sub>2</sub> nanotubes (NTs) on the electrode plate were grown by anodic oxidation of titanium substrate and then decorated by a low loading of silver nanoparticles deposited by sputtering (i.e. Ag/TiO<sub>2</sub> NTs). Due to their quasi one-dimensional arrangement, TiO<sub>2</sub> NTs are able to provide higher surface area for Ag adhesion and superior electron transport properties than other Ti substrates (e.g. Ti foil and TiO<sub>2</sub> nanoparticles), as confirmed by electrochemical (CV, EIS, electrochemical active surface area) and chemical/morphological analysis (FESEM, TEM, EDS). These characteristics together with the role of the TiO<sub>2</sub> NTs to enhance the stability of CO<sub>2</sub> intermediate formed due to titania redox couple (Ti<sup>IV</sup>/Ti<sup>III</sup>) lead to an improvement of the CO production in the Ag/TiO<sub>2</sub> NTs electrodes. Particular attention has been devoted to reduce the loading of noble metal in the electrode (14.5 %w/%w) and to increase the catalysts active surface area in order to decrease the required overpotential.

© 2019 Hydrogen Energy Publications LLC. Published by Elsevier Ltd. All rights reserved.

## Introduction

Carbon dioxide is recognized to be one of the main contributions to Global Warming and its reuse is currently considered a key challenge to the current society [1]. In addition, our energy system mainly rely on non-sustainable fuels like oil and coals, which might be depleted in the near future [2]. In the last decades, different strategies have been considered to

overcome these global challenges; from Carbon Capture and Storage (CCS) to the exploitation of renewable energies to reuse carbon dioxide and obtain added-value products. CCS can contribute to reduction of CO<sub>2</sub> emission level but at a significant costs [3].

Recently, the conversion of CO<sub>2</sub> to added-value products has gained a lot of attention in the scientific community [4,5]. Among all the proposed methods to handle this problem,

\* Corresponding author.

\*\* Corresponding author.

E-mail addresses: [amin.farkhondehfal@iit.it](mailto:amin.farkhondehfal@iit.it) (M.A. Farkhondehfal), [simelys.hernandez@polito.it](mailto:simelys.hernandez@polito.it) (S. Hernández).

<https://doi.org/10.1016/j.ijhydene.2019.04.180>

0360-3199/© 2019 Hydrogen Energy Publications LLC. Published by Elsevier Ltd. All rights reserved.

electrochemical reduction of CO<sub>2</sub> is an attractive solution from both economic and environmental points of view [6]. However, the industrial utilization of CO<sub>2</sub> to fuel is currently under development. Clearly emphases have been given to increase the current low efficiency and low production rate. In fact, depending on the selected catalyst, reaction conditions and electrolyte, different products such as carbon monoxide [7–9], formic acid [10,11], hydrocarbon including methane or methanol [12,13] or mixtures of them can be obtained. Moreover, the CO<sub>2</sub> is typically dissolved in aqueous media and, consequently, the hydrogen evolution reaction (HER) is in inevitable competition with the CO<sub>2</sub> reduction. Therefore, a competitive approach regards the combined CO<sub>2</sub> reduction and HER for the production of syngas, which consists of a mixture of H<sub>2</sub> and CO (in different ratios), given the robust options for downstream processing to generate more reduced products via Fischer-Tropsch heterogeneous catalysis [6]. Indeed, syngas is an important intermediate for production of chemicals like acetic acid (carbonylation) [14], aldehydes (Hydroformylation) [15] and also many light and heavy chained carbon fuels and alcohols (Fischer & Tropsch) [16].

Theoretically, in an aqueous media, CO<sub>2</sub> can be electrochemically reduced to CO with a potential difference of 1.335 V vs NHE (at pH 7, 25 °C, 1 atm gas pressure, 1 M for solutes), considering O<sub>2</sub> evolution at the anode; but, in general, more negative potentials have to be applied to initiate the CO<sub>2</sub> reduction [17]. Because of these high overpotentials and low productivity, large improvements are required to make this process viable for large-scale industrialization. Electrocatalysts that simultaneously exhibit a low overpotential, high faradaic efficiency and high productivity toward the desired products have to be developed [18].

Over the last decade, various catalysts have been used for electrochemical reduction of CO<sub>2</sub> to CO (and syngas when using an aqueous electrolyte media) [7,19–25]. Hori et al. have tested different metals as electrocatalyst for that purpose and concluded that Au and Ag are the most active ones. Due to its lower cost, Ag has gained more attention than Au and has been used in different forms and configurations: from bulk to nanoparticles, and with different co-catalysts or supported on different substrates [7,19,26–30]. In addition, one of the major barriers in the electrochemical reduction of CO<sub>2</sub> is known to be the formation of CO<sub>2</sub><sup>•-</sup> radical that is the a rate determining step for reduction of CO<sub>2</sub> and implies high overpotentials in the applied system [31]. Different approaches have been explored to tackle this issue, for instance, the use of ionic liquids like 1-ethyl-3-methylimidazolium tetrafluoroborate (EMIM-BF<sub>4</sub>) [20] and Pyrazolium [32] as co-catalyst for Ag cathode which, however, resulted in low current densities of –5 mA/cm<sup>2</sup> and –45 mA/cm<sub>2</sub> (in a relatively high applied potential of –2.4 V vs Fc), respectively, or, more recently, the use of triangular Ag nano plates to achieve a low overpotential of 97 mV, but obtained an even lower current density of –1.25 mA/cm<sup>2</sup> than in the previous works [33].

To date, most of the research has been focused on the electrocatalyst for CO<sub>2</sub> reduction reaction (CO<sub>2</sub>-RR) whereas few works explored the role of the co-catalyst in this reaction. For example, Tornow et al. investigated four different N-based organometallics catalysts with Ag [34]. They found that a Ag-based 3,5-diamino-1,2,4-triazole supported on carbon

(AgDAT/C) produced about –70 mA cm<sup>–2</sup> of current density with almost 90% of Faradaic efficiency for the production of CO. Sastre et al. also reported the effect of graphitic carbon nitride as a co-catalyst of nano-structured Ag for syngas production [29].

In this work, titania nanotubes (TNT) have been used for the first time as an active support for Ag nanoparticles (Ag NPs) with the aim to increase both the electrochemical active surface area of the catalyst and to take advantage of the titania's ability in facilitating the CO<sub>2</sub> reduction process. Previously, Cueto et al. reported the effect of Ag NPs deposited on TiO<sub>2</sub> thin film for reduction of CO<sub>2</sub> [35]. However, the focus of that report was in the surface characterization and not in the productivity and selectivity of the catalyst and the effect of TiO<sub>2</sub> in the CO<sub>2</sub> reactivity. Moreover, Ag-modified TiO<sub>2</sub> nanocatalyst has been used for photo-induced CO<sub>2</sub> reduction by hydrogen for selective CO evolution [36]. In another work, Ma et al. investigated the role of TiO<sub>2</sub> NPs (the commercial Aeroxide TiO<sub>2</sub> P25) as the substrate for Ag NPs deposition for electroreduction of CO<sub>2</sub> to CO by using different Ag loadings from 5% to 40 wt% [26]. They proposed that CO<sub>2</sub> is absorbed on titania and then it gains one electron to form CO<sub>2</sub><sup>•-</sup> radical, which is stabilized in the TiO<sub>2</sub> surface, resulting in lower overpotentials. As a result, in that work they obtained a current density of about 100 mA/cm<sup>2</sup>, with a high faradaic efficiency of 90% towards CO, by using the 40% Ag/TiO<sub>2</sub> catalyst. It is noteworthy to mention that this high current density has been achieved in a Rotating Disk Electrode (RDE) in a very small-scale size electrode (0.07 cm<sup>2</sup> of area), which not necessarily can be extrapolated to a bigger scale due to different mass transfer phenomena.

The uniqueness of this work is that we investigated the role of Titania nanotubes as a co-catalyst for Ag nano particles, which are being sputtered in low quantities with the aim to develop a highly efficient and cheap electrocatalyst for the reduction of CO<sub>2</sub> into syngas. The reported material has been thoroughly analyzed both morphologically and electrochemically to understand the role of 1D vertically aligned TiO<sub>2</sub> nanotubes in improving the kinetics and mass transfer for the CO<sub>2</sub>RR.

## Experimental

### Catalyst preparation

TiO<sub>2</sub> nanotubes (NTs) were prepared as follows. Titanium foil (Alfa Aesar, Titanium foil 0,25 mm thick, annealed, 99,5% pure, 4 cm<sup>2</sup>) was sandblasted and etched by the solution of HF (wt.40%, Sigma Aldrich) for 1 min to remove the native oxide layer obtaining a fresh metal surface for the NTs growth and then the TiO<sub>2</sub> nanotubes were synthesized by anodization method in a 0,5 wt% NH<sub>4</sub>F (98%, Sigma Aldrich) and 2,5 wt% H<sub>2</sub>O in ethylene glycol (98%, Sigma Aldrich) electrolyte at 60 V [37]. After 10 min, the synthesized nanotubes are removed by sonication in H<sub>2</sub>O<sub>2</sub> (40%, Sigma Aldrich) solution. The anodization procedure was repeated for other 10 min. In this way, well organized TiO<sub>2</sub> nanotubes can be grown in the footprint of previously removed ones. After cleaning the NTs arrays with DI-Water and ethanol to

remove the residual of electrolyte, they were calcined at 450 °C for 1 h in ambient pressure.

For the preparation of TiO<sub>2</sub> nanoparticle-based electrode a titanium foil (Alfa Aesar, Titanium foil 0,25 mm thick, annealed, 99,5% pure) was sandblasted and rinsed by ethanol and a layer of 30 µm of TiO<sub>2</sub> paste (Dyesol, 18NR-T Titania paste) was deposited by doctor blade technique on the foil. The TiO<sub>2</sub> layer was then dried at 100 °C for 30 min and calcined at 525 °C for 1 h in ambient atmosphere.

For the deposition of Ag nanoparticles (NPs) a sputter coater (Quorum Q150T ES) equipped with a Ag target (Testbourne Ltd, S5-9000-D35 Silver Target 99,99% pure) has been used to prepare a set of catalyst samples with different Ag NPs loadings, which depend on the sputtering conditions (current and time) as reported in Table 1. The notation used to name the catalyst contains the kind of substrate, i.e. Titania nanotubes (TNT) and the Ag sputtering conditions, i.e. 60 mA and 90s. In addition, to investigate the effect of Titania nanotubes (TNT) on electrochemical reduction of CO<sub>2</sub>, two other Ti-based substrates: Titania nanoparticles (TNP) and Titanium foil (Ti foil), were used to compare their performance with respect to the TNT-based samples, with Ag nanoparticles deposited under the same conditions.

### Electrochemical test

The electrochemical tests of the Ag NPs were done in a three electrodes reactor by using a Pt electrode (99.9% metals basis, Sigma–Aldrich) as anode, a 2.4 cm<sup>2</sup> electrode (from the ones in Table 1) as working electrode in the cathode and a saturated Calomel electrode (SCE, Radiometer analytical) all being controlled by a potentiostat (Autolab, PGSTAT302 N). The two compartments of the reactor were separated by a Nafion 115 membrane. The scheme of this system can be seen in Figure S-1.

For comparison of the behavior of different TiO<sub>2</sub> and Ag substrates, electrochemical analyses were done in a one compartment reactor, by using the same electrodes configuration of the two-compartment reactor. As electrolyte, a solution of 0.1 M KHCO<sub>3</sub> was prepared by adding the proper amount of Millipore water to dissolve KHCO<sub>3</sub> (P9144 Sigma-Aldrich > 99.5%). In both cases, the reactor was bubbled with a continuous flow of CO<sub>2</sub> to maintain the electrolyte saturated with it and the composition of the exit gas was analysed with an Inficon MicroGC.

The electrochemical techniques which have been carried out are Cyclic Voltammetry (CV, scan rate of 20 mV/s), Linear Sweep Voltammetry (LSV), Chronoamperometry (CA, 90 min for

each applied potentials), Electrochemical Impedance Spectroscopy (EIS) and finally Electrochemical Active Surface Area analysis (ECSA) using Capacitance measurement method.

### Characterization

A ZEISS Auriga field emission scanning electron microscope (FESEM) was used to characterize the morphology of the electrocatalysts and the substrate as well as to evaluate the dispersion and dispersion of Ag nanoparticles on the TiO<sub>2</sub>. In addition for quantifying the amount of Ag, Energy Dispersive X-Ray spectroscopy (EDX) technique has been used as illustrated in Figure S-2 & 9. A PANalytical X'Pert Xray diffractometer (XRD) was used to study the crystalline phases and the surface composition. The X-ray source used was a Cu K $\alpha$  monochromatic radiation ( $\lambda = 1,54 \text{ \AA}$ ). Also, a FEI Tecnai F20ST transmission electron microscopy (TEM), operating at 220 kV, was employed to study the morphology of the catalyst.

## Results and discussion

The developed electrocatalysts are composed of Ag nanoparticles deposited by sputtering on Titania nanotubes grown on a Ti foil. The major advantage of using sputtering for the deposition of Ag nanoparticles is the adjustability to spread nano-sized Ag particles on the substrate in a more homogeneous way and with a low and controlled amount of catalyst precursor. The amount of deposited Ag nanoparticles was tuned by applying different currents and deposition times as shown in Table 1 (see Experimental section). The electrochemical tests are reported in two sections. First, in section [Influence of Ag sputtering conditions on TiO<sub>2</sub> NTs on the electrochemical CO<sub>2</sub>RR](#), the performance of electrodes prepared with different sputtering conditions were screened with the aim to find the best ones for the reduction of CO<sub>2</sub> to CO. Then, in section [Influence of pressure on the electrochemical CO<sub>2</sub>RR with the Ag/TNT sample](#), the real effect of Titania NTs is investigated by comparing the optimum loading of Ag NPs on different Ti-based substrates.

### Influence of Ag sputtering conditions on TiO<sub>2</sub> NTs on the electrochemical CO<sub>2</sub>RR

Fig. 1 shows a FESEM image of the synthesized TiO<sub>2</sub> NTs, which have grown perpendicular and well oriented on the Ti foil, with a compact shape and a length of 2.8–3 µm and an

**Table 1 – List of synthesized catalyst.**

Catalyst name	Catalyst nature	Sputtering current and time	Ag loading (w/w %) <sup>a</sup>
20 mA-90s	Ag/TiO <sub>2</sub> nanotubes	20 mA, 90 s	3.5
40 mA-90s	Ag/TiO <sub>2</sub> nanotubes	40 mA, 90 s	8.2
60 mA-90s or Ag/TNT	Ag/TiO <sub>2</sub> nanotubes	60 mA, 90 s	14.5
80 mA-90s	Ag/TiO <sub>2</sub> nanotubes	80 mA, 90 s	24.2
Ag/Ti foil	Ag/Ti foil	60 mA, 90 s	N/A
Ag/TNP	Ag/TiO <sub>2</sub> nanoparticles	60 mA, 90 s	N/A
TNT	TiO <sub>2</sub> nanotubes	No silver	–
Ti foil	Ti foil	No silver	–

<sup>a</sup> The method for measuring the Ag loading has been described in SI ([Figure S-9](#)).



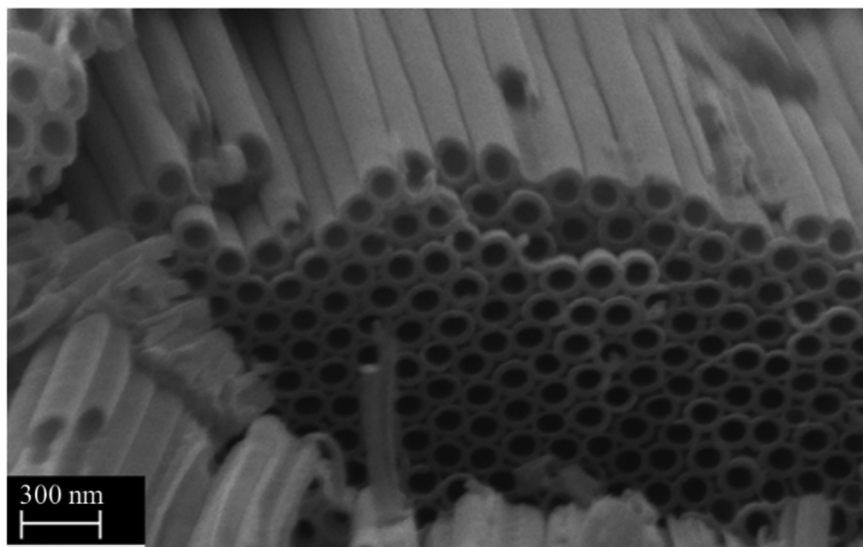


Fig. 1 – FESEM image of Titania nanotubes.

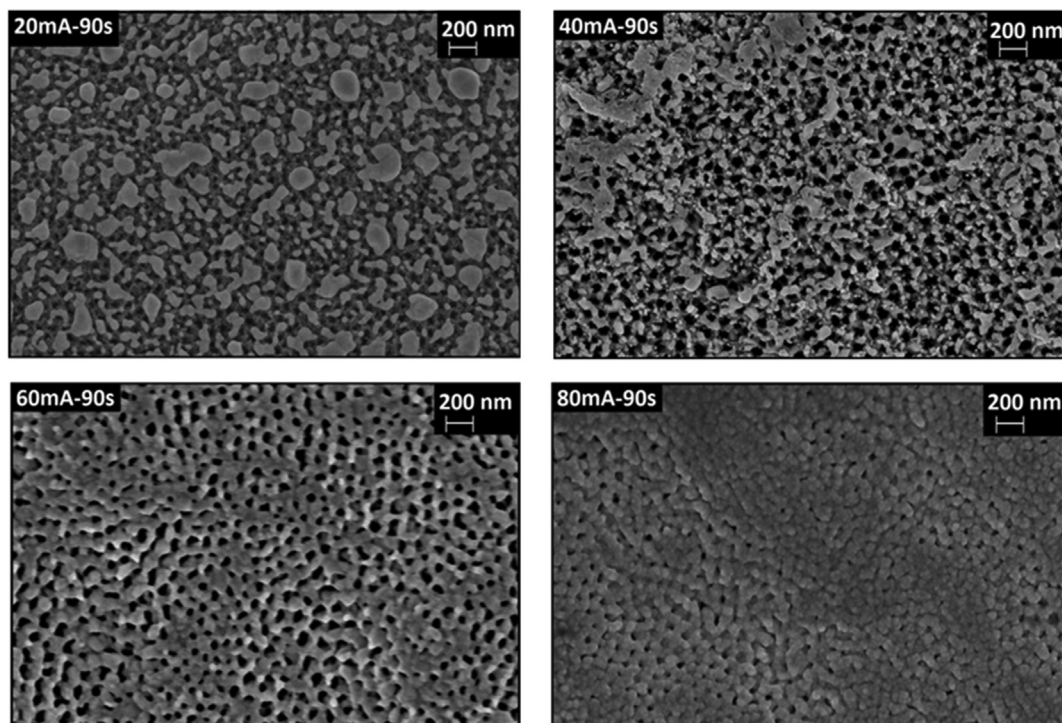


Fig. 2 – Top-view FESEM images of Ag-deposited Titania nanotubes by sputtering for 90s with different applied currents of 20, 40, 60 and 80 mA.

individual diameter of 80–100 nm. The effect of changing the sputtering current was in the coverage by Ag nanoparticles of the TNT as shown in the top-view FESEM images in Fig. 2, in which the electrodes prepared with 90 s of deposition time at four different currents (i.e. 20, 40, 60 and 80 mA) are reported. As expected, the higher the applied current for sputtering was, the higher was the coverage and agglomeration of Ag nanoparticles. Although an increase of the sputtering current was expected to improve the coverage by Ag of the TNT substrate, at the current of 80 mA the Ag nanoparticles covered the

whole TNTs surface, completely carpeting their mouth, which could make the application of TNT in this process almost useless.

Moreover, as can be seen in the TEM side view of the prepared Ag sputtered Titania nanotube at 60 mA/90s (see Fig. 3) Ag nanoparticles have covered the surface of Titania nanotubes and they did not penetrate completely inside the nanotubes.

To quantify the productivity of the prepared Ag/TiO<sub>2</sub> NTs electrocatalysts, a series of chronoamperometry tests have

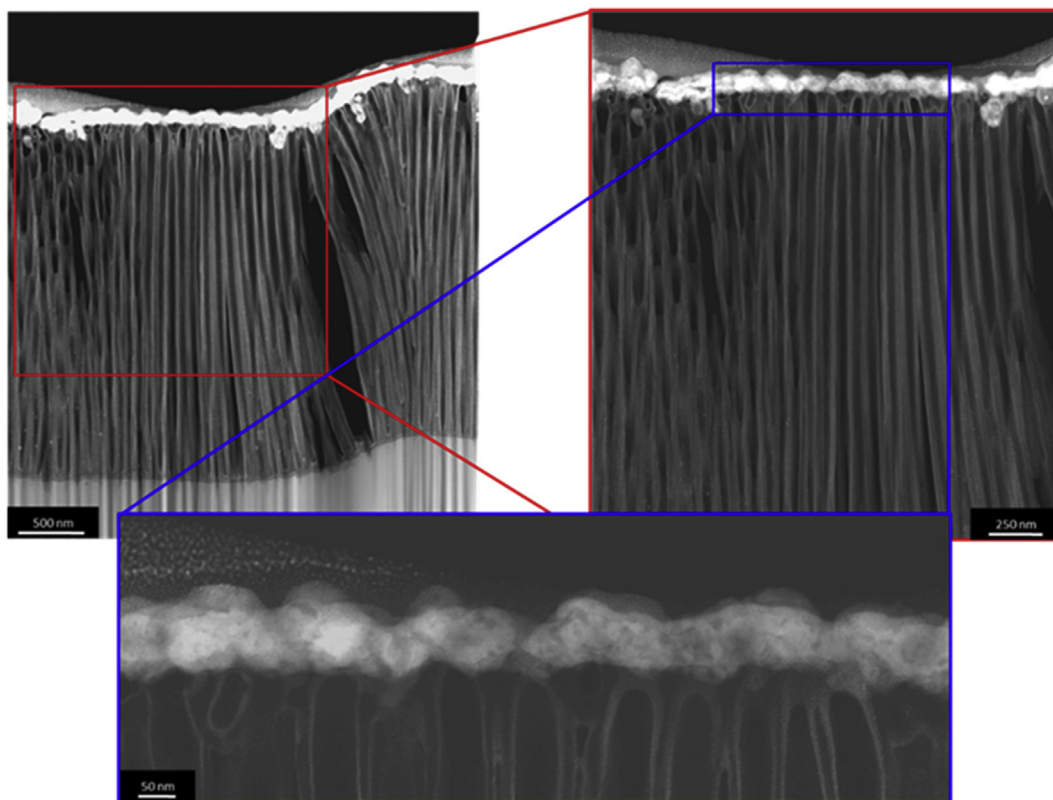


Fig. 3 – TEM side view image of 60 mA 90s before the reaction.

been done at 3 different applied potentials:  $-1.4$  V,  $-1.5$  V and  $-1.6$  V vs SHE, in a two-compartment cell. The CO production rate and the CO/H<sub>2</sub> ratio was measured after steady-state conditions (90 min) at each potential and the results are reported in Fig. 4. From Fig. 4a it is evident that, at  $-1.4$  and  $-1.5$  vs SHE, the 80 mA-90s sample showed to be the best electrode among the others for CO production most probably as a result of higher Ag loading. However, since the tests were done in sequence by increasing the applied potential, this catalyst evidenced a decay of performance (Figure S-4) at  $-1.6$  V vs. SHE in comparison to the 60 mA-90s sample. Indeed, the 60 mA-90s electrode showed the best performance at  $-1.6$  V vs. SHE by producing a higher amount of CO than the other catalysts and also higher durability over the time although

generally all the electrocatalysts have lost some of their activity over the time (see Figure S-5).

Moreover, to investigate the effect of coverage of Ag nanoparticles on electrochemical active surface area (ECSA) of the catalyst, a measurement based on double-layer capacitance was done. Usually, to measure it, cyclic voltammetry (i-V) curves are recorded in the mere double layer region at various scan rates. Then, the current in the middle of the potential vs. scan rate window is taken and plotted against the respective scan rate and a straight line should result, whose slope is an indicative value of the ECSA of the catalyst relative to a reference flat electrode of the same material, as indicated in following:

$$i = dQ/dt = (dQ/dE) \cdot (dE/dt) = C \cdot V \quad (1)$$

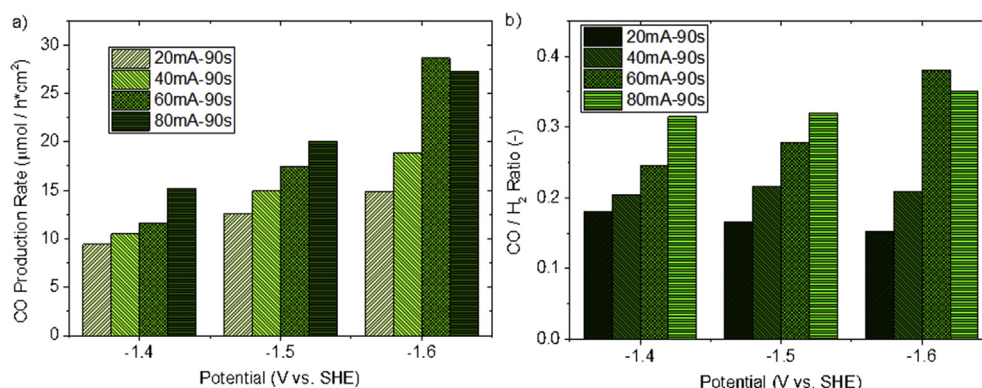


Fig. 4 – a) CO production rate b) CO to H<sub>2</sub> ratio in 3 different potentials.

where,  $i$  is current (A),  $Q$  is charge (C),  $E$  is potential (V) and  $C$  is capacitance.

ECSA can be calculated by referring the obtained capacitance to the reference value per the unit area ( $C_{ref}$ );

$$ECSA_{rel} = C / C_{ref} \quad (2)$$

Thus, by comparing the slope of the current vs. scan rate in the double layer capacitance zone, the value of  $ECSA_{rel}$  of the different prepared catalysts can be distinguished. The  $ECSA_{rel}$  values were calculated before and after the chronoamperometric tests at all the potentials. In general, a higher slope indicates a higher ECSA of the material, considering to have a constant reference capacitance ( $C_{ref}$ ) value. As shown in Fig. 5 at the beginning of the electrochemical  $CO_2$  reduction reaction, the higher the amount of Ag resulted in higher  $ECSA_{rel}$  but this trend changed after the reaction. This indicates that the surface properties of the electrodes changed during the electrochemical tests and can be also used as an indication of the different durability of the catalysts. The 80 mA-90s sample evidenced the highest  $ECSA_{rel}$  at the beginning of the tests. However, at the end of the reaction (after 4hr of tests) the  $ECSA_{rel}$  of the 60 mA-90s sample was the highest, followed by the 40mA-90s electrode. This behavior can be explained by an agglomeration and growth in size of the active Ag nanoparticles which are the main catalyst for  $CO_2$  reduction to CO, as can be seen in Fig. 6. This phenomenon, was evidently enhanced in the samples with a higher Ag loading, as can be observed by the higher difference in  $ECSA_{rel}$  before and after the  $CO_2RR$  of the 80 mA-90s samples than for the 20 mA-90s one.

For a further analysis of the durability of the catalysts, which is important to maintain the CO production rates over time, and to understand if the Ag agglomeration is the only explanation for the decrease of the  $ECSA_{rel}$  over the time, the Ag loading of the electrodes was measured before and after the chronoamperometric test. It is clear from Fig. 7 that some Ag was lost from the electrodes surface, which was confirmed by ICP analyses on the electrolyte that reveals the existence of

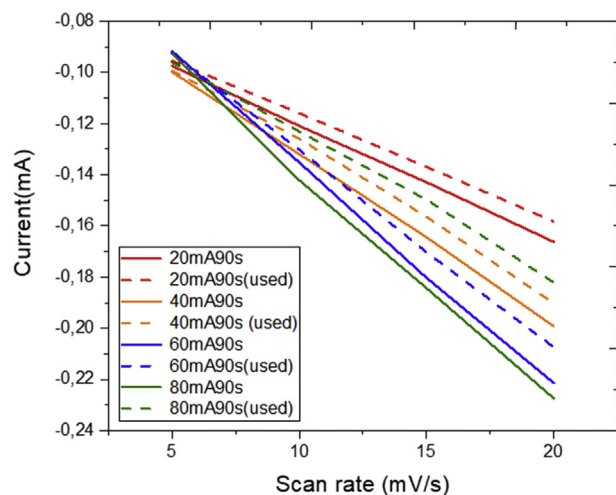


**Fig. 5 – ECSA ratio for different catalyst before (lines) and after (dotted lines) the  $CO_2RR$ .**

some ppm of Ag ( $\leq 2\%$ W/W) in the electrolyte after the  $CO_2RR$ . It is evident from Fig. 7 that the percentage of loss of Ag from the catalyst surface is higher in the samples with a lower Ag loading (of about 35% and 30% for the 20 mA-90s and 40 mA-90s samples, respectively), which is in agreement with the decrease of activity and  $ECSA_{rel}$  of these electrocatalyst. Instead, for the Ag/TNT electrodes with a higher Ag loading (i.e. 60 mA-90s and 80 mA-90s) that lost less amounts of Ag, the main reason for the loss of activity and ECSA of the catalyst seems to be the agglomeration of Ag nanoparticles, which then causes a reduction of the catalytically active surface. Although from the FESEM and  $ECSA_{rel}$  results, the Ag agglomerations and leaching seem to be more significant for the 80 mA-90s sample which resulted in a lowering of the activity and durability of this sample. In contrast, the 60 mA-90s sample reported the best stability among the here reported electrocatalysts (the Ag lost was lower than 5% and the CO production rate decrease of less than 10% in the 20 h of test). Anyhow the decay in the electrocatalytic activity of all the electrodes can be caused by membrane fouling to some extent.

In previous literature reports for  $CO_2RR$  to CO, i.e. about 70% of published works, the stability of the electrocatalyst is often not reported or it is proved for less than 3 h of continuous reaction [16]. Therefore, it is important to investigate the reasons of catalyst instability.

Based on FESEM,  $ECSA_{rel}$  gravimetric and ICP results, one can conclude that the Ag NPs agglomeration could be explained due to a difference in charge of Ag particles with different sizes, as already reported in literature [38] and that is schematized in Fig. 8. In fact, it has been observed that larger Ag particles has a partial negative charge and smaller particles have a partial positive charge at electrical equilibrium, due to the greater work function of the larger particles [38]. Thus, at the surface of an electrocatalyst, the larger nanoparticle accepts an electron from a neighboring smaller particle through the conducting substrate. In that moment, the smaller nanoparticle becomes more positively charged and reestablishes equilibrium by dissolving an  $Ag^+$  ion into solution. The result is an agglomeration of bigger Ag particles and dissolution of smaller Ag nanoparticles (a kind of Ostwald ripening) [38]. This hypothesis agrees with the partial dissolution and reduction of Ag loading (Fig. 7) and with the reshaping and agglomeration of Ag particles shown in FESEM images (Fig. 6) observed for the electrodes after the reaction. As can be seen in Fig. 6, some of Ag nanoparticles are attached to each other and agglomerated in a huge cubic form. Others seems to be detached and scattered in different parts of the surface, which could be due to  $Ag^+$  dissolution and re-deposition on the electrode surface. It is noteworthy that EDS and XRD analysis also confirmed the nature of this agglomerated cubes to be Ag (Figure S-2&3).

Additionally, TEM analysis were done after the  $CO_2RR$  with the 60 mA-90s sample and TEM images shown in Fig. 9 confirmed the reshaping of Ag nanoparticles with respect to the sample before the test (shown in Fig. 3). The scattering and reshaping of Ag particles, apart from a re-orientation of the superficial Ag in the top of the  $TiO_2$  NTs, also caused some Ag particles to be re-deposited into the inner surface of the  $TiO_2$  NTs (see Figs. 8 and 9).



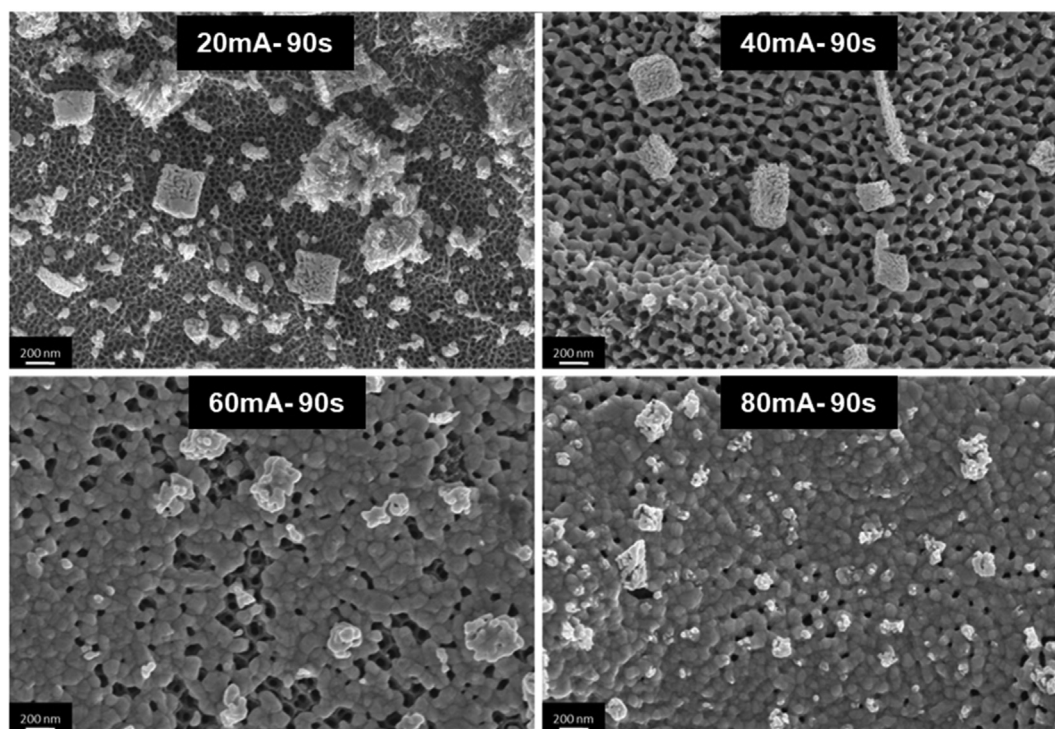


Fig. 6 – FESEM top view of Ag sputtered electrocatalyst after 4hr of reaction.

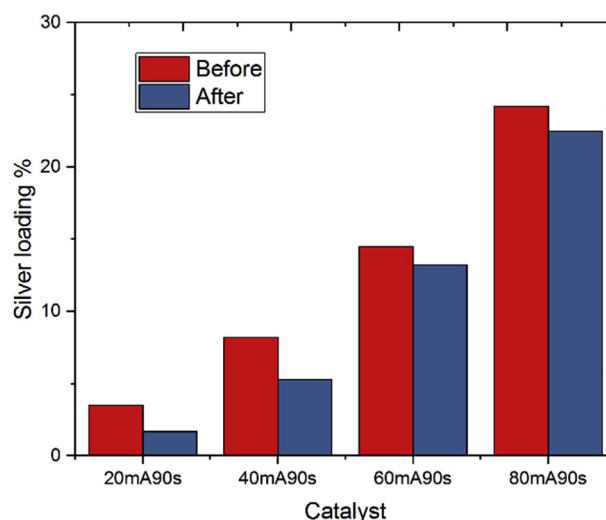
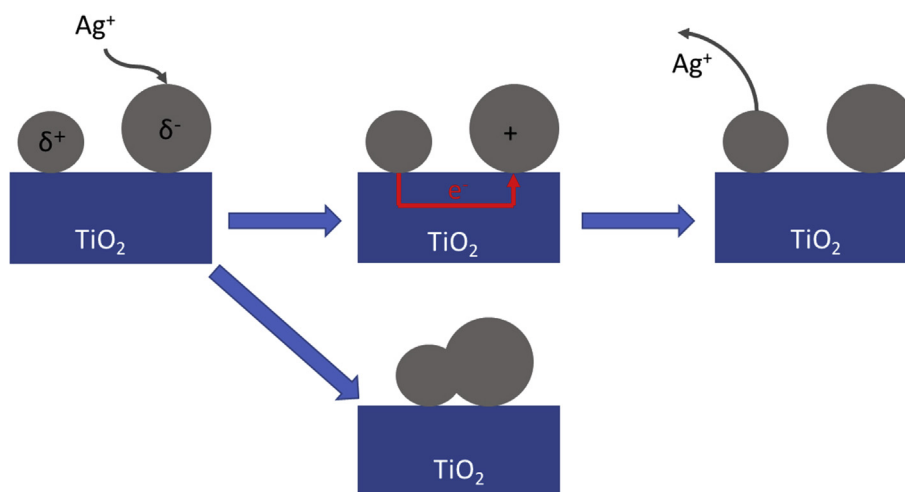


Fig. 7 – Ag loading for different catalyst measured before and after reaction.

#### *Influence of pressure on the electrochemical CO<sub>2</sub>RR with the Ag/TNT sample*

Another parameter that can improve the performance for the electrochemical reduction of CO<sub>2</sub> is pressure. The reason is that the amount of CO<sub>2</sub> dissolved in aqueous electrolyte increases by increasing the pressure of CO<sub>2</sub> in the reactor. Hence, to reduce in some extent the mass transfer limitations due to CO<sub>2</sub> dissolution and to investigate the effect of pressure on the performance of the best of the Ag/TNT electrodes, we performed an additional chronoamperometric experiment

under CO<sub>2</sub>RR conditions by increasing the pressure of the reactor to 7 atm. A comparison between CO and H<sub>2</sub> production rates at 1 and 7 atm, at the different applied potentials, are reported in the bar graphs in Fig. 10. As expected, the CO production rate was increased in this second experiment, however, this increase was more clear at the lower potentials (i.e. it was doubled at  $-1.4$  V and  $-1.5$  V vs SHE), in which the CO<sub>2</sub> reduction reaction is evidently more dominant than the H<sub>2</sub> evolution reaction (HER, which also increased but in a lower proportion). In comparison, at  $-1.6$  V vs SHE the CO productivity was only increased by about 20% and the HER



**Fig. 8 – Schematic mechanism of agglomeration and/or dissolution of Ag ions into the electrolyte.**

dramatically raised in about 45%. These results demonstrate that (i) the CO/H<sub>2</sub> ratio can be strongly affected by the working pressure at a specific applied potential and that (ii) these two parameters have to be tuned in function of the desired final production between CO and H<sub>2</sub>. As an example, at 1.4 V vs SHE the ratio of quasi 1:2 (CO:H<sub>2</sub>) obtained which is an ideal ratio for syngas to be used as a feedstock for methanol production.

Furthermore, to measure the maximum current density which can be achieved by the electrocatalyst, one should remove all the barriers which prevents the electrons to pass through from the surface of the catalyst to electrolyte and

finally reduce the dissolved CO<sub>2</sub>. The major barrier to this phenomenon is mass transfer diffusion resistance in electrolyte. One way to minimize this effect is to use rotating disk as working electrode. As the disk turns, some of the solution described as the hydrodynamic boundary layer is dragged by the spinning disk and the resulting centrifugal force flings the solution away from the center of the electrode. Hence, solution flows up, perpendicular to the electrode, from the bulk to replace the boundary layer. The sum result is a laminar flow of solution towards and across the electrode. The rate of the solution flow can be controlled by the electrode's angular velocity

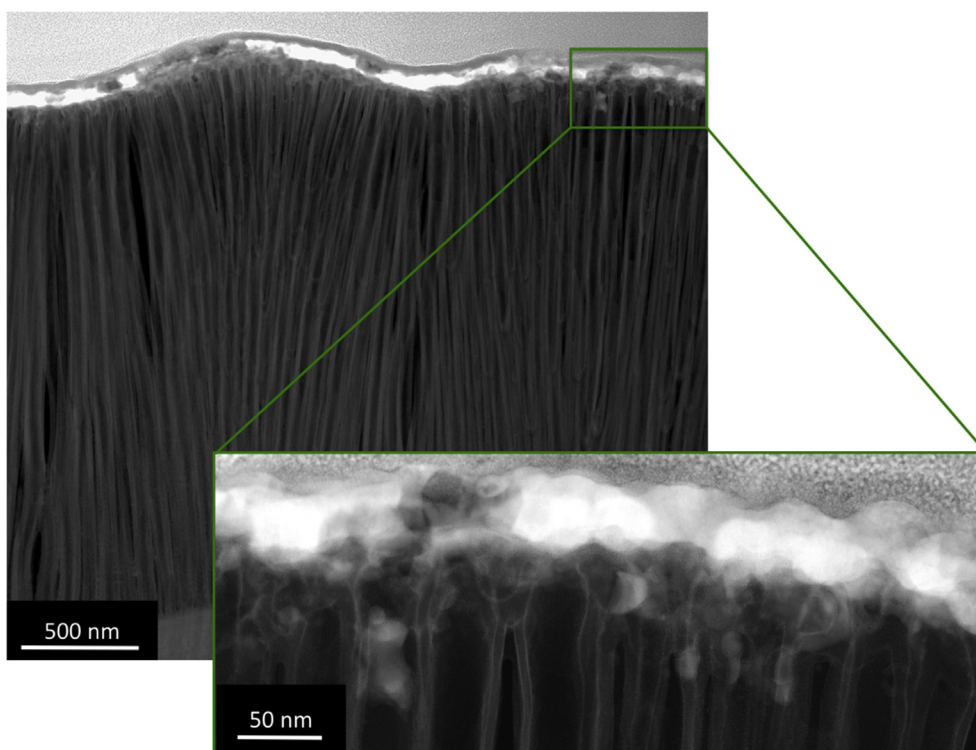


**Fig. 9 – TEM side view image of 60 mA 90s after the reaction.**

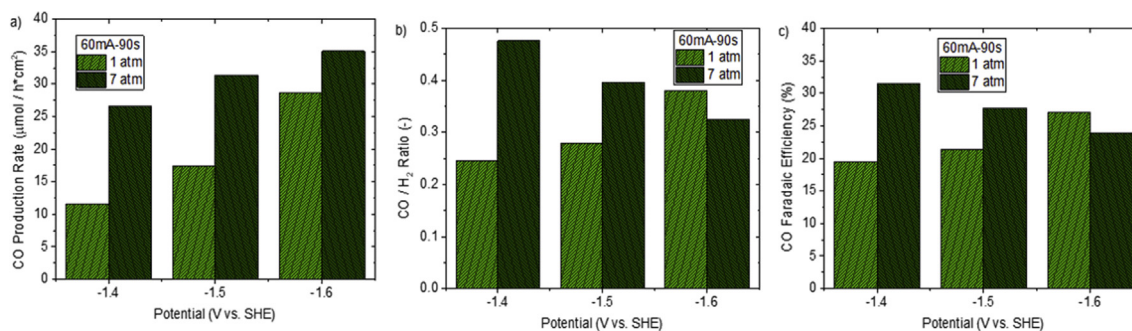


Fig. 10 – a) CO production rate b) CO to H<sub>2</sub> ratio and c) CO Faradaic efficiency at 1 and 7 atm.

and modeled mathematically. This flow can quickly achieve conditions in which the steady-state current is controlled by the solution flow rather than diffusion [39]. This is a contrast to the more stagnant flow (classical) experiments where the steady-state current is limited by the diffusion of species in solution. For this reason, an LSV (linear sweep voltammetry) has been done in a RDE with 1600 rpm using 60 mA-90s in the same electrolyte of KHCO<sub>3</sub> 0.1 M. Initially, LSV test has been done with N<sub>2</sub> bubbling and then the electrolyte saturated by CO<sub>2</sub> and the same test has been repeated. As can be seen in Fig. 11 a higher onset potential can be noticed when CO<sub>2</sub> reduction is occurring, which can be as a result of formation of CO<sub>2</sub><sup>-</sup> radical which has its own kinetical barrier compared to the process with only HER (blue line). When the applied potential increases the current density increases drastically respect to the reaction without CO<sub>2</sub>. This difference in current densities can be attributed to CO<sub>2</sub>-RR. It is noteworthy that the highest current density for CO<sub>2</sub> reduction achieved at -1.6 V vs SHE with -65 mA/cm<sup>2</sup> which can be considered quite high

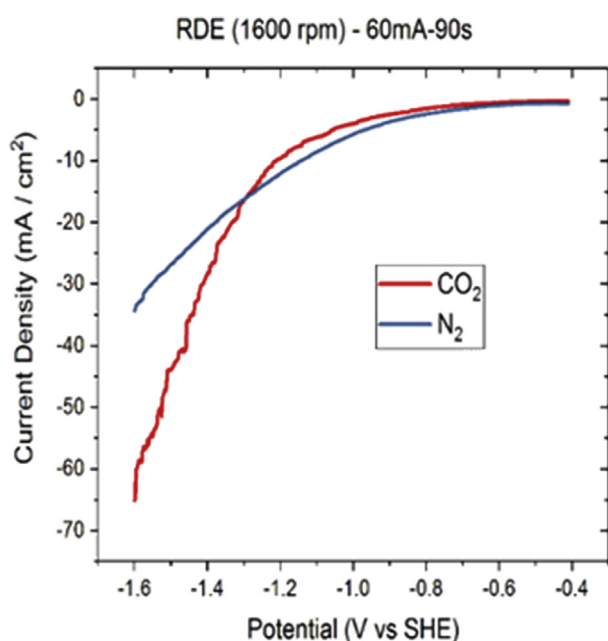


Fig. 11 – LSV test in RDE for Ag/TNT 60 mA 90s with N<sub>2</sub> bubbling (blue) and CO<sub>2</sub> bubbling. (For interpretation of the references to colour in this figure legend, the reader is referred to the Web version of this article).

with respect to the experiments which have been carried out by bulk noble metal electrodes [7,29,40]. A comparison of the most recent result for syngas production can be found in Tables S–3 in the supporting information.

### Role of titania nanotubes on the electrochemical CO<sub>2</sub>RR

To investigate the actual effect of the titania nanotubes in electrocatalytic activity of Ag NPs for the CO<sub>2</sub>RR the optimized sputtering conditions (60 mA and 90s) has been used for Ag deposition on different substrates: Titania NTs on Ti foil, Titania NPs on Ti foil and bare Ti foil. These electrodes were tested in a single chamber cell and the results obtained in continuous under steady-state conditions at three different potentials (see Experimental section) are reported in Fig. 12. The analysis of the products of the above-mentioned catalysts showed that TiO<sub>2</sub> is not an electrocatalyst for CO<sub>2</sub> reduction; in fact, the CO productivity obtained with this material (in both electrodes: TNT and TiO<sub>2</sub> NPs on Ti foil) was almost zero and overlaps with the behavior of the Ti foil at all the studied potentials (Fig. 12a). Indeed, TiO<sub>2</sub> has been mainly used as a support for Ag (and other noble metals like Au and Pt) to reduce CO<sub>2</sub> into CO or other C-based compounds under photocatalytic conditions [41,42]. The use of TiO<sub>2</sub> NPs as a support for a Ag electrocatalyst has only been reported in a previous work [26], in which the participation of Ti<sup>IV</sup>/Ti<sup>III</sup> was attributed to acts as the redox couple that stabilizes the CO<sub>2</sub>RR intermediate. Moreover, the trivalent titanium in TiO<sub>2</sub> reported to serve as an efficient site for adsorption of CO<sub>2</sub> and stabilization of the adsorbed CO<sub>2</sub><sup>-</sup> radical. Consequently, the reduction of CO<sub>2</sub> on TiO<sub>2</sub>NTs electrodes involves a fast first electron and proton transfer followed by a slow second proton transfer as the rate-limiting step [43].

This argument can be confirmed by analyzing the productivity of the above-mentioned catalysts. As shown in Fig. 12, at the three applied potentials, the Ag/TNT catalyst showed the best performance. It is worth noticing that, at -1.4 V vs SHE both the electrodes with Ag deposited on the TiO<sub>2</sub> substrates demonstrated a superior CO productivity than the Ag/Ti foil electrode. At the higher potentials, due to detachment of Ag nanoparticles from the TiO<sub>2</sub> NPs substrate, the catalytic activity of this electrode drastically decreased; instead, the Ag NPs on the TiO<sub>2</sub> NTs demonstrated to be more stable than on the TiO<sub>2</sub> NPs. As already observed in the previous tests, although the production of CO increases by increasing the potential, the CO/H<sub>2</sub> ratio decreases because the HER prevails over the CO<sub>2</sub>RR under these conditions.

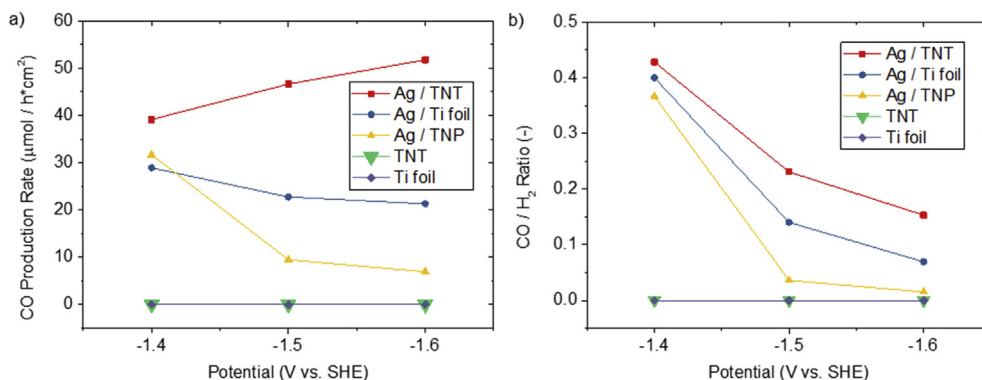


**Fig. 12 – a) CO production rate b) CO to H<sub>2</sub> ratio for Ag nanoparticles as the catalyst with different substrate in different potentials.**

Electrochemical impedance spectroscopy (EIS) measurements have also been carried out to investigate in more depth the effect of TiO<sub>2</sub> NTs as Ag substrate for the CO<sub>2</sub>RR and the results are shown in Fig. 13. At a first glance, it appears that the impedance related to the Ag/Ti foil sample is quite large with respect to the other two samples, in agreement with the results discussed above. In addition, also the shape of the spectrum in the low frequency region is quite different. In fact, usually the typical spectrum of an electrode immersed in an electrolytic solution during an electroreduction process is characterized by a high frequency feature (i.e. a leftmost arc). This process at high frequencies is related to the faster process, i.e. charge transfer at the electrode-electrolyte interface. Then, the lower frequency arc is related to the slower process, which could account for the Warburg diffusion [44]. The high frequency process, which is related to the extent of the electroreduction can be modeled through a parallel between the charge transfer resistance R<sub>1</sub> and the double layer capacitance C<sub>1</sub>, while the low frequency one, which accounts for the mass

transport limitations, can be modeled through a Warburg impedance, characterized by the resistance R<sub>2</sub>; the series resistance R<sub>s</sub> models the ohmic losses (Figure S-8) [45]. It is noteworthy that for the mass transport limitation a Warburg Short element has been used. This element is the extension of Warburg element to represent the finite length diffusion, i.e. where no bulk electrolyte condition is present in the analyzed system [46]. The equivalent circuit composed by these elements was used to fit the experimental impedance data: the fitting procedure was proved to be good for the electrode based on titanium oxide (see the solid curves in Fig. 13), while gave origin to not reliable results when used for Ti foil-based electrode. The reason for the observed discrepancy can be attributed to the supposed capability of TiO<sub>2</sub> to stabilize the reaction intermediates, which favors the CO<sub>2</sub> electroreduction: this characteristic is not evidenced in Ti foil, thus causing a double layer formation at the Ti/Ag interface, which limits the overall reaction. This hypothesis is supported by the fact that a good fitting can be obtained by substituting the Warburg impedance with a low frequency double layer process, characterized by a resistance R<sub>2</sub> and a capacitance C<sub>2</sub> (see Figure S-8b): the curve calculated using this model is

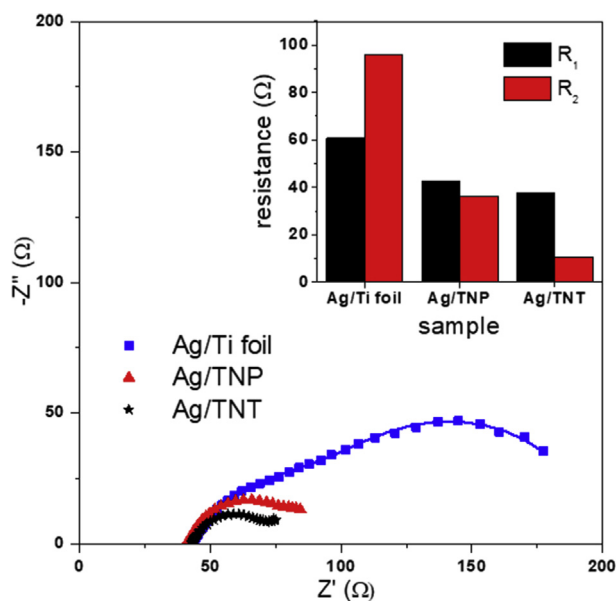


**Fig. 13 – EIS analysis for 3 different substrates with the same Ag loading.**

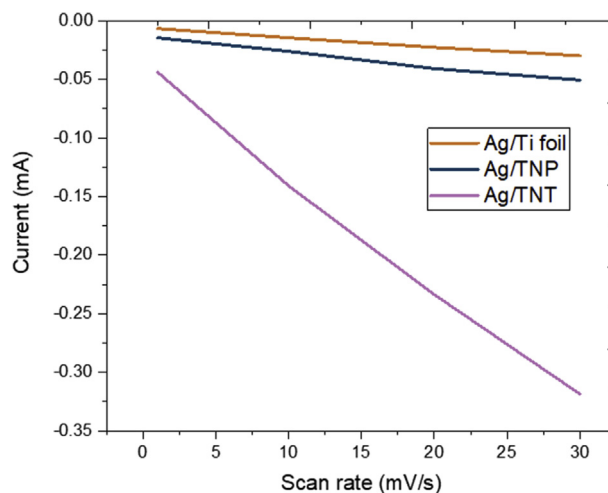


**Fig. 14 – The ECSA ratio measurement for electrocatalysts with different Ti substrates.**



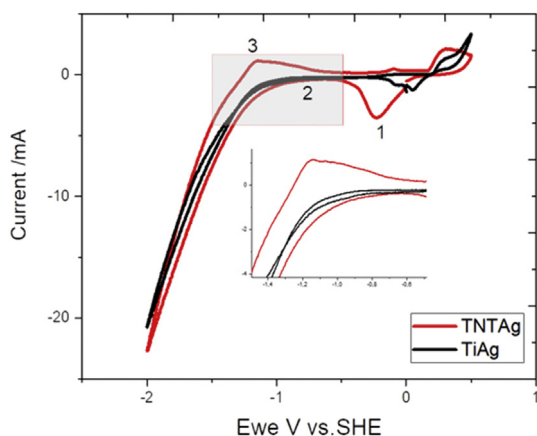


**Fig. 15 – Cyclic voltammetry of Ag/Ti foil and Ag/TNT in the presence of CO<sub>2</sub>.**

reported in Fig. 13 (blue curve). The values of the resistances obtained through the fitting procedure are reported in the inset of Fig. 13; as it demonstrates, the Ag/Ti foil sample is characterized by larger resistances, and the low frequency process becomes the limiting step of the reaction. On the contrary, the Ag/TNT electrode exhibits the lowest impedance, due to the fast electron path provided by the TiO<sub>2</sub> NTs mono-dimensional structuration.

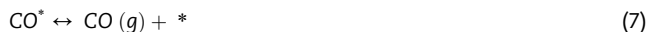
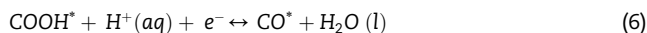
Furthermore, ECSA<sub>rel</sub> has been measured (as described above) for the Ag deposited on the different substrates by comparing the slope of the current vs. scan rate data after different CV tests in the double layer capacity zone. Evidently from Fig. 14 the slope for ECSA<sub>rel</sub> for the sample with Ag NPs deposited on TiO<sub>2</sub> NTs is by far larger than those of the others. It can, therefore, be concluded that Ag NPs being deposited on Titania nanotubes have a higher electrochemical active surface area than the same kind of Ag NPs deposited on both Ti foil and titania NPs. These analyses confirm once more the role of Titania nanotubes as the substrate for Ag nanoparticles to improve the performance of electrocatalyst.

The outcomings of both the EIS and ECSA studies confirm that the TiO<sub>2</sub> NTs are able to improve electrons transport and catalytically active surface area of electrocatalyst for the CO<sub>2</sub>RR, in agreement with previous studies in which this material has been used as substrate for metal oxide catalysts for other electrochemical applications [47,48]. This is due to the increase in the active surface area and stabilizing the rate determining radicals by facilitating the electron transfer route [26].

Moreover, in order to understand the role of Titania nanotubes in the process of CO<sub>2</sub> reduction into CO by Ag nanoparticles, it is noteworthy to present the mechanism of CO<sub>2</sub> on Ag electrode. According to Kortlever et al. [49], the reaction pathway for electroreduction of CO<sub>2</sub> to form CO on Ag electrodes consists of these following steps<sup>1</sup>:



<sup>1</sup> The \* sign represents the adsorption status on the surface of electrode.



The first initial steps can occur either as a one-step Proton Coupled Electron Transfer (equation (3)) or two step mechanism (equations (4) and (5)). An interesting recent work by Firet et al. [50], confirmed these mechanism by monitoring the thin film Ag electrode by operando attenuated reflectance Fourier transformed infrared spectroscopy (ATR-FTIR). Based on this proposition, by applying higher potentials the mechanism changes from a one-step PCET in to a two-steps reaction. In both high and low overpotentials the formation of COO<sup>-\*</sup> (CO<sub>2</sub><sup>-ads</sup>) for the CO production is very significant.

In addition, DFT calculations by Yangt et al. [51], showed that the presence of Ag NPs can substantially modify CO<sub>2</sub> adsorption on anatase TiO<sub>2</sub> (101). This calculation suggested that Ag particles affect the CO<sub>2</sub> adsorption on TiO<sub>2</sub> sites where there is no binding between CO<sub>2</sub> and the particle itself, which can be described as a form of modification of properties of TiO<sub>2</sub> as it donates electron density to the surface [51]. In another words, the substantial amount of electrons which are being transferred from the interface of electrode-electrolyte to CO<sub>2</sub> molecules and causing the formation of activated CO<sub>2</sub><sup>-</sup> anions and eventually enhanced the CO<sub>2</sub>RR activity.

In order to compare the above proposed mechanism with electrochemical behavior of Ag-decorated Titania nanotubes, a comparison of cyclic voltammetry of TNT/Ag and Ti/Ag with CO<sub>2</sub> bubbling has been done so one can differentiate the mechanism of CO<sub>2</sub> reduction. As has been shown in Fig. 15 the major difference in CV between using Ti and TNT are the existence of the reduction peaks numbered as 1 and 3 that can be attributed to the reactions for TiO<sub>2</sub> (Ti<sup>IV</sup>) and Ti<sup>III</sup> species, which can indeed act as a redox electron carrier to facilitate the electrochemical reaction steps, which include CO<sub>2</sub> reduction [5]. For this reason the trivalent titanium in TiO<sub>2</sub> reported to serve as an efficient site for stabilization of the adsorbed CO<sub>2</sub><sup>-</sup> radical [43]. Moreover, this hydroxylation of Titania cluster has been said to be accounted for CO<sub>2</sub> reduction conditions in aqueous environment. As a result, DFT calculations showed a strong bonding between CO<sub>2</sub> and hydroxylate species on Titania surface, which causes a significant bending from linear CO<sub>2</sub> to a tridentate formation of O-C-O that facilitates the subsequent CO<sub>2</sub> transformations [52]. In addition, based on the comparison of LSV's with Nitrogen bubbling and CO<sub>2</sub> bubbling (Fig. 11) potential value numbered as 2 in Fig. 15 can be described as the onset potential for the CO<sub>2</sub>RR, which in case of the Ag/TNT electrode happened at a lower overpotential than on the Ag/Ti foil sample. This description confirms the redox behavior of Ti<sup>IV</sup>/Ti<sup>III</sup> for CO<sub>2</sub> ads. reduction to CO<sub>2</sub><sup>-ads</sup>. This redox couple can facilitate the transfer of electron for PCET mechanism to create redox radicals (COO<sup>-</sup> and COOH<sup>\*</sup> for the formation final reduction products).

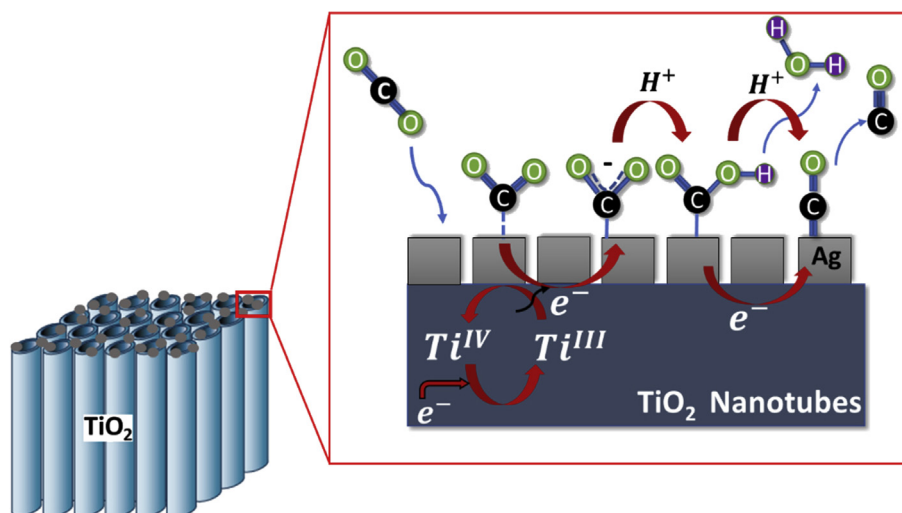


Fig. 16 – The schematic of the mechanism of CO<sub>2</sub> reduction over Ag-decorated Titania nanotube in aqueous electrolyte.

This analysis confirms the proposed mechanism of Ag-decorated Titania nanotube for electrocatalytic reduction of CO<sub>2</sub> to CO shown in Fig. 16. As has been discussed before, by passing electrons through titania nanotubes, the redox couple is created by which electron transfer to adsorbed is facilitated to create CO<sub>2</sub><sup>•-</sup> radical and then at the presence of Ag nanoparticles this radical will be reduced to CO molecule.

## Conclusion

In the presented work Ag-decorated titania nanotube has been used for the electrocatalytic reduction of CO<sub>2</sub> for the production of syngas. Among different Ag loadings, the electrocatalyst with sputtered silver at applied currents of 60 mA for 90 s of deposition time showed to have a best performance and stability among other low Ag loading titania nanotubes. Furthermore, the role of titania in facilitating the process of CO<sub>2</sub> reduction has been investigated: it is argued that TiO<sub>2</sub> probably is involved in the adsorption and stabilization of the CO<sub>2</sub><sup>•-</sup> radical intermediate, which then can react to form CO on adjacent Ag particles. Nanotubes showed to outperform Ag-decorated titania nanoparticles by increasing the electrochemical active surface area by achieving a molar ratio of CO/H<sub>2</sub> of 1:2 which is a perfect proportion for the feedstock for the methanol production. The morphological analysis of Ag-supported titania nanotubes showed the re-shaping of Ag particles during the reaction caused by possible acceptance of electron from a neighboring smaller Ag particle through the conducting substrate and causing agglomeration of Ag particles and dissolution of Ag + into electrolyte. As a consequence, a decrease in the electrocatalytic activity of Ag nanoparticles by both loss of Ag particles and decrease in the active surface area of agglomerated Ag particles have been found. In general, this work opens new doors for using nanostructures titania as a support for (silver based) electrocatalyst in CO<sub>2</sub> reduction. The stability of the electrocatalyst and production rate of syngas are, however, still a challenge that needs to be resolved to achieve the scale up targets for

electrocatalytic reduction of CO<sub>2</sub> to syngas at an industrially relevant scale.

## Appendix A. Supplementary data

Supplementary data to this article can be found online at <https://doi.org/10.1016/j.ijhydene.2019.04.180>.

## REFERENCES

- [1] Roy SC, Varghese OK, Paulose M, Grimes CA. Toward solar fuels: photocatalytic conversion of carbon dioxide to hydrocarbons. *ACS Nano* 2010;4(3):1259–78.
- [2] Olah GA, Goeppert A, Prakash GKS. Chemical recycling off carbon dioxide to methanol and dimethyl ether: from greenhouse gas to renewable, environmentally carbon neutral fuels and synthetic hydrocarbons. *J Org Chem* 2009;74(2):487–98.
- [3] Verma S, Lu X, Ma SC, Masel RI, Kenis PJA. The effect of electrolyte composition on the electroreduction of CO<sub>2</sub> to CO on Ag based gas diffusion electrodes. *Phys Chem Chem Phys* 2016;18(10):7075–84.
- [4] Jhong HR, Ma SC, Kenis PJA. Electrochemical conversion of CO<sub>2</sub> to useful chemicals: current status, remaining challenges, and future opportunities. *Current Opin Chem Eng* 2013;2(2):191–9.
- [5] Ma SC, Perez GMJ, Moniri S, Kenis PJA. Support materials for catalysts for electrochemical reduction of CO<sub>2</sub> to value added products. *Abstr Pap Am Chem Soc* 2013:246.
- [6] Jones JP, Prakash GKS, Olah GA. Electrochemical CO<sub>2</sub> reduction: recent Advances and current trends. *Isr J Chem* 2014;54(10):1451–66.
- [7] Delacourt C, Ridgway PL, Kerr JB, Newman J. Design of an electrochemical cell making syngas (CO+H<sub>2</sub>) from CO<sub>2</sub> and H<sub>2</sub>O reduction at room temperature. *J Electrochem Soc* 2008;155(1):B42–9.
- [8] DiMeglio JL, Rosenthal J. Selective Conversion of CO<sub>2</sub> to CO with high efficiency Using an inexpensive Bismuth-based electrocatalyst. *J Am Chem Soc* 2013;135(24):8798–801.

- [9] Hori Y, Takahashi R, Yoshinami Y, Murata A. Electrochemical reduction of CO at a copper electrode. *J Phys Chem B* 1997;101(36):7075–81.
- [10] Chen YH, Li CW, Kanan MW. Aqueous CO<sub>2</sub> Reduction at very low Overpotential on oxide-derived Au nanoparticles. *J Am Chem Soc* 2012;134(49):19969–72.
- [11] Zhang S, Kang P, Ubnoske S, et al. Polyethylenimine-enhanced electrocatalytic reduction of CO<sub>2</sub> to formate at nitrogen-doped carbon nanomaterials. *J Am Chem Soc* 2014;136(22):7845–8.
- [12] Cole EB, Lakkaraju PS, Rampulla DM, Morris AJ, Abelev E, Bocarsly AB. Using a one-electron shuttle for the multielectron reduction of CO<sub>2</sub> to methanol: Kinetic, mechanistic, and structural insights. *J Am Chem Soc* 2010;132(33):11539–51.
- [13] Seshadri G, Lin C, Bocarsly AB. A new homogeneous electrocatalyst for the reduction of carbon-dioxide to methanol at low overpotential. *J Electroanal Chem* 1994;372(1–2):145–50.
- [14] Sunley GJ, Watson DJ. High productivity methanol carbonylation catalysis using iridium - the Cativa (TM) process for the manufacture of acetic acid. *Catal Today* 2000;58(4):293–307.
- [15] Schulz H. Short history and present trends of Fischer-Tropsch synthesis. *Appl Catal Gen* 1999;186(1–2):3–12.
- [16] Hernandez S, Farkhondehfar MA, Sastre F, Makkee M, Saracco G, Russo N. Syngas production from electrochemical reduction of CO<sub>2</sub>: current status and prospective implementation. *Green Chem* 2017;19(10):2326–46.
- [17] Rong J, Bosserez T, Martel D, et al. Monolithic cells for solar fuels. *Chem Soc Rev* 2014;43(23):7963–81.
- [18] Whipple DT, Kenis PJA. Prospects of CO<sub>2</sub> utilization via direct heterogeneous electrochemical reduction. *J Phys Chem Lett* 2010;1(24):3451–8.
- [19] Kim B, Ma S, Jhong HRM, Kenis PJA. Influence of dilute feed and pH on electrochemical reduction of CO<sub>2</sub> to CO on Ag in a continuous flow electrolyzer. *Electrochim Acta* 2015;166:271–6.
- [20] Rosen BA, Salehi-Khojin A, Thorson MR, et al. Ionic liquid-mediated selective Conversion of CO<sub>2</sub> to CO at low overpotentials. *Science* 2011;334(6056):643–4.
- [21] Thorson MR, Siil KI, Kenis PJA. Effect of cations on the electrochemical conversion of CO<sub>2</sub> to CO. *J Electrochem Soc* 2013;160(1):F69–74.
- [22] Kauffman DR, Alfonso DR, Tafen DN, et al. Selective electrocatalytic reduction of CO<sub>2</sub> into CO at small, thiol-capped Au/Cu nanoparticles. *J Phys Chem C* 2018;122(49):27991–8000.
- [23] Chen P, Jiao Y, Zhu Y-H, et al. Syngas production from electrocatalytic CO<sub>2</sub> reduction with high energetic efficiency and current density. *J Mater Chem* 2019;7(13):7675–82.
- [24] Lv K, Teng C, Shi M, et al. Hydrophobic and electronic properties of the E-MoS<sub>2</sub> nanosheets induced by FAS for the CO<sub>2</sub> electroreduction to syngas with a wide range of CO/H<sub>2</sub> ratios. *Adv Funct Mater* 2018;28(49):1802339.
- [25] Marques Mota F, Nguyen DLT, Lee J-E, et al. Toward an effective control of the H<sub>2</sub> to CO ratio of syngas through CO<sub>2</sub> electroreduction over immobilized gold nanoparticles on layered titanate nanosheets. *ACS Catal* 2018;8(5):4364–74.
- [26] Ma SC, Lan YC, Perez GMJ, Moniri S, Kenis PJA. Silver supported on titania as an active catalyst for electrochemical carbon dioxide reduction. *ChemSusChem* 2014;7(3):866–74.
- [27] Ma SC, Luo R, Gold JI, Yu AZ, Kim B, Kenis PJA. Carbon nanotube containing Ag catalyst layers for efficient and selective reduction of carbon dioxide. *J Mater Chem* 2016;4(22):8573–8.
- [28] Salehi-Khojin A, Jhong HRM, Rosen BA, et al. Nanoparticle silver catalysts that show enhanced activity for carbon dioxide electrolysis. *J Phys Chem C* 2013;117(4):1627–32.
- [29] Sastre F, Muñoz-Batista MJ, Kubacka A, et al. Efficient electrochemical production of syngas from CO<sub>2</sub> and H<sub>2</sub>O by using a nanostructured Ag/g-C<sub>3</sub>N<sub>4</sub> catalyst. *Chem Electrochem* 2016;3(9):1497–502.
- [30] Yu Y, Zhong N, Fang J, et al. Comparative study between pristine Ag and Ag foam for electrochemical synthesis of syngas with carbon dioxide and water. *Catalysts* 2019;9(1).
- [31] Hori Y. Handbook of fuel cells. Wiley; 2010.
- [32] Vasilyev D, Shirzadi E, Rudnev AV, Broekmann P, Dyson PJ. Pyrazolium ionic liquid Co-catalysts for the electroreduction of CO<sub>2</sub>. *ACS Appl Energy Mater* 2018;1(10):5124–8.
- [33] Subiao Liu HT, Li Z, Qi L, Xu Z, Liu Q, Jing-Li L. Shape-dependent electrocatalytic reduction of CO<sub>2</sub> to CO on triangular silver nanoplates. *J Am Chem Soc* 2017;139:4.
- [34] Tornow CE, Thorson MR, Ma S, Gewirth AA, Kenis PJA. Nitrogen-based Catalysts for the electrochemical Reduction of CO<sub>2</sub> to CO. *J Am Chem Soc* 2012;134(48):19520–3.
- [35] Cueto LF, Martinez GT, Zavala G, Sanchez EM. Surface characterization and CO<sub>2</sub> reduction using electrodeposited silver particles over TiO<sub>2</sub> thin film. *J Nano Res* 2010;9:89–100.
- [36] Tahir M, Amin NAS. Photo-induced CO<sub>2</sub> reduction by hydrogen for selective CO evolution in a dynamic monolith photoreactor loaded with Ag-modified TiO<sub>2</sub> nanocatalyst. *Int J Hydrogen Energy* 2017;42(23):15507–22.
- [37] Lamberti A, Chiodoni A, Shahzad N, Bianco S, Quaglio M, Pirri CF. Ultrafast room-temperature crystallization of TiO<sub>2</sub> nanotubes exploiting water-vapor treatment. *Sci Rep* 2015;5.
- [38] Redmond PL, Hallock AJ, Brus LE. Electrochemical Ostwald ripening of colloidal Ag particles on conductive substrates. *Nano Lett* 2005;5(1):131–5.
- [39] Naughton MS, Moradia AA, Kenis PJA. Quantitative analysis of single-electrode plots to understand in-situ behavior of individual electrodes. *J Electrochem Soc* 2012;159(6):B761–9.
- [40] Dufek EJ, Lister TE, Stone SG, McIlwain ME. Operation of a pressurized system for continuous reduction of CO<sub>2</sub>. *J Electrochem Soc* 2012;159(9):F514–7.
- [41] Li Y, Wang WN, Zhan ZL, Woo MH, Wu CY, Biswas P. Photocatalytic reduction of CO<sub>2</sub> with H<sub>2</sub>O on mesoporous silica supported Cu/TiO<sub>2</sub> catalysts. *Appl Catal B Environ* 2010;100(1–2):386–92.
- [42] Zhang Q-H, Han W-D, Hong Y-J, Yu J-G. Photocatalytic reduction of CO<sub>2</sub> with H<sub>2</sub>O on Pt-loaded TiO<sub>2</sub> catalyst. *Catal Today* 2009;148(3):335–40.
- [43] Qiu J-P, Tong Y-W, Zhao D-M, He Z-Q, Chen J-M, Song S. Electrochemical reduction of CO<sub>2</sub> to methanol at TiO<sub>2</sub> nanotube electrodes. *Acta Physico-Chim Sin* 2017;33(7):1411–20.
- [44] Delmondo L, Salvador GP, Munoz-Tabares JA, et al. Nanostructured Mn<sub>x</sub>O<sub>y</sub> for oxygen reduction reaction (ORR) catalysts. *Appl Surf Sci* 2016;388:631–9.
- [45] Chang KW, Ji W, Kaun CC. Layer-separable and gap-tunable topological insulators. *Phys Chem Chem Phys* 2017;19(5):3932–6.
- [46] Sacco A. Electrochemical Impedance spectroscopy: fundamentals and application in dye-sensitized solar cells. *Renew Sustain Energy Rev* 2017;79:15.
- [47] Momeni MM, Ghayeb Y, Ghonchehi Z. Fabrication and characterization of copper doped TiO<sub>2</sub> nanotube arrays by in situ electrochemical method as efficient visible-light photocatalyst. *Ceram Int* 2015;41(7):8735–41.
- [48] Kowalski D, Mallet J, Thomas S, et al. Electrochemical synthesis of 1D core-shell Si/TiO<sub>2</sub> nanotubes for lithium ion batteries. *J Power Sources* 2017;361:243–8.
- [49] Kortlever R, Shen J, Schouten KJP, Calle-Vallejo F, Koper MTM. Catalysts and reaction pathways for the electrochemical reduction of carbon dioxide. *J Phys Chem Lett* 2015;6(20):4073–82.

- [50] Fiet NJ, Smith WA. Probing the reaction mechanism of CO<sub>2</sub> electroreduction over Ag films via operando infrared spectroscopy. *ACS Catal* 2017;7(1):606–12.
- [51] Yang CT, Wood BC, Bhethanabotla VR, Joseph B. CO<sub>2</sub> adsorption on anatase TiO<sub>2</sub> (101) surfaces in the presence of subnanometer Ag/Pt clusters: implications for CO<sub>2</sub> photoreduction. *J Phys Chem C* 2014;118(45):26236–48.
- [52] Chu S, Ou P, Ghamari P, et al. Photoelectrochemical CO<sub>2</sub> reduction into syngas with the metal/oxide interface. *J Am Chem Soc* 2018;140(25):7869–77.